

# J80-095 Stability Aspects of Diverging Subsonic Flow

Michael C. Cline\*

*University of California, Los Alamos, New Mex.*

Flow instability occurs when calculating subsonic, internal, inviscid, diverging flow using a time-dependent method. This instability and its relation to the numerical method, boundary conditions, and viscous effects are analyzed both analytically and numerically. The inviscid flow is shown to be physically unstable as well as a poor representation of the true viscous flow.

## I. Introduction

**T**HIS paper describes the computation of two-dimensional, subsonic, diverging, internal flows and how they differ from the corresponding converging flows. Such diverging or decelerating flows occur in such obvious places as subsonic diffusers and inlets. However, such flows also occur in supersonic nozzles when a normal shock is present.

To illustrate the problem, consider the case of planar sink flow shown in Fig. 1. The region to be computed is enclosed by dashed lines. The upper boundary is assumed to be a free-slip solid wall, and the lower boundary is the flow midplane. The flow, from left to right, is a converging or accelerating flow. The midplane inflow Mach number is 0.16 and the outflow value is 0.5. The numerical solution for this flow as well as all flows considered here was calculated using the VNAP code.<sup>1</sup> The Mach number contours for this case are shown in Fig. 2 for four time step  $N$  values. The  $N=0$  plot corresponds to the one-dimensional solution used as an initial estimate, whereas  $N=3000$  corresponds to the steady-state two-dimensional solution. There is  $<1.0\%$  difference between the numerical and the exact solution.

Now consider the case of planar source flow shown in Fig. 3. The midplane inflow Mach number is 0.5 and the outflow value is 0.16. The Mach number contours for this case are shown in Fig. 4. Figure 4 shows that the source flow did not converge to the exact solution as did the sink flow. Instead, the computation becomes unstable and finally causes the pressure to go negative at  $N=1593$ . It is the cause of this instability and its consequences that are the subject of this paper.

## II. Numerical Method

The VNAP code solves the two-dimensional, time-dependent, compressible Navier-Stokes equations. The fluid is assumed to be a perfect gas. The interior grid points are computed using the second-order-accurate MacCormack finite-difference scheme. The free-slip wall, subsonic inflow, and outflow boundary grid points are calculated using a second-order-accurate reference plane characteristic scheme. The no-slip wall and midplane boundary grid points are computed using the MacCormack scheme with one-sided differences normal to the boundary. For details of the method see Ref. 1.

The inviscid source and sink flows were computed with zero viscosity and thermal conductivity (Euler equations) as well as the free-slip wall boundary condition. Source flow

calculations also were made with nonzero viscosity and conductivity (Reynolds number of 100) and the free-slip wall boundary condition. However, these results did not differ qualitatively from the inviscid results. In addition, the MacCormack scheme is not known to have any stability problems for subsonic flows where there are no shocks, local sonic points, or stagnation points. The inflow and outflow boundary schemes, based on the method of characteristics, have been used to compute many subsonic, inviscid and viscous flows<sup>1</sup> with no numerical stability problems. Despite this, several different inflow and outflow boundary schemes based on extrapolation and reflection were tried with no improvement. Therefore, because of no anticipated numerical stability problems and the fact that the sink flow calculation produced excellent results, we believe that the source flow instability is not due to the numerical method.

## III. Boundary Conditions

Our next objective was to determine whether the boundary conditions used here result in a well-posed problem. Therefore, this section contains a discussion of the boundary conditions for two-dimensional, subsonic, inviscid, unsteady flow. The emphasis is to describe the important facts, without resorting to equations and mathematical analysis. The desire is to trade off some mathematical rigor for clarity. The additional boundary conditions due to the presence of viscous terms are not discussed here but can be found in the paper by Olinger and Sundström.<sup>2</sup>

The boundary conditions used for both the source and sink flows specify the  $x$ -direction velocity component  $u$ , the  $y$ -direction velocity component  $v$ , the density  $\rho$  at the inflow boundary, and the pressure  $p$  at the outflow boundary. The actual values used are the sink and source flow exact solution.

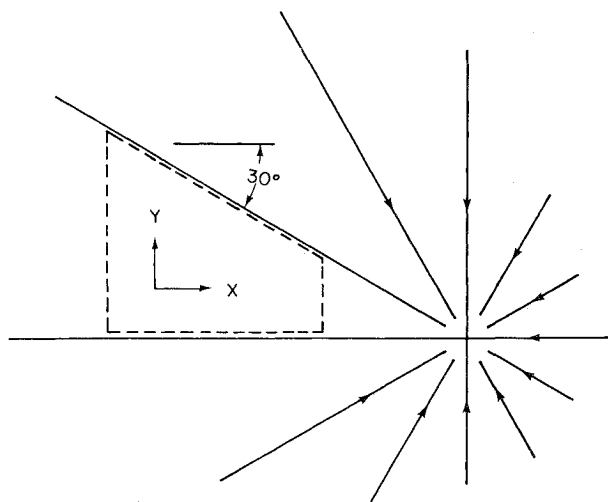


Fig. 1 Planar sink flow.

Received May 21, 1979; revision received Sept. 25, 1979. This paper is declared a work of the U.S. Government and therefore is in the public domain. Reprints of this article may be ordered from AIAA Special Publications, 1290 Avenue of the Americas, New York, N.Y. 10019. Order by Article No. at top of page. Member price \$2.00 each, nonmember, \$3.00 each. **Remittance must accompany order.**

Index categories: Boundary Layer Stability and Transition; Subsonic Flow; Computational Methods.

\*Group T-3, Los Alamos Scientific Laboratory. Member AIAA.

20004  
20005  
20016

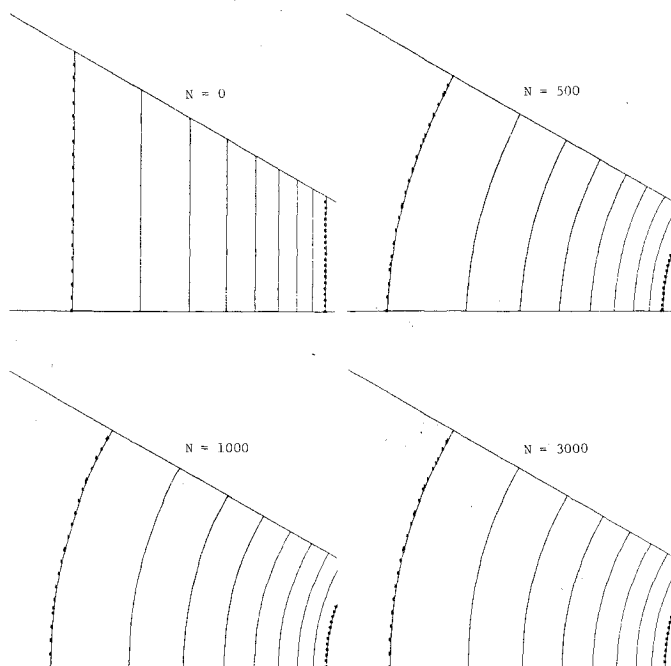


Fig. 2 Mach number contours for the planar sink flow case.

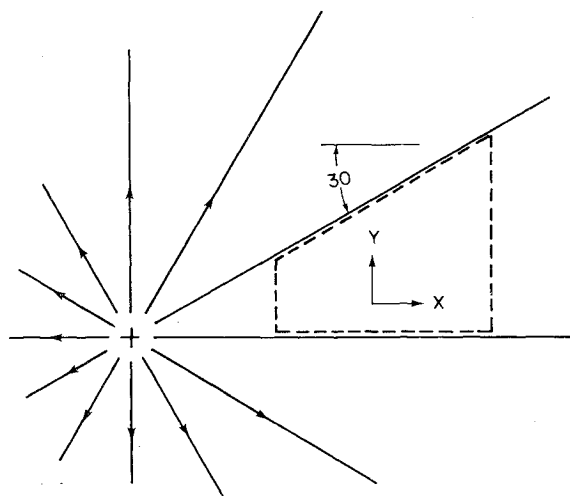


Fig. 3 Planar source flow.

The free-slip wall and midplane boundary used the vanishing of the normal velocity component and flow symmetry, respectively, as the boundary conditions. Using  $u$ ,  $v$ , and  $p$  at the subsonic inflow boundary and  $p$  at the subsonic outflow boundary was shown to be well posed by Olinger and Sundström.<sup>2</sup>

The time-dependent inviscid equations are hyperbolic, so the same boundary conditions can be determined by characteristic theory. The partial differential equations for time-dependent, inviscid, compressible flow are hyperbolic and, therefore, can be written in characteristic form. Characteristic form means that the original equations can be written as an equal number of equations, called compatibility equations, that apply along certain lines, called bicharacteristics or simply characteristics. The number of characteristics is less than or equal to the number of original equations. The number of boundary conditions equals the number of compatibility equations on incoming characteristics, that is, characteristics that enter the computational region for positive time. The form of the boundary conditions may be determined from the fact that the compatibility equations along outgoing characteristics (those that couple

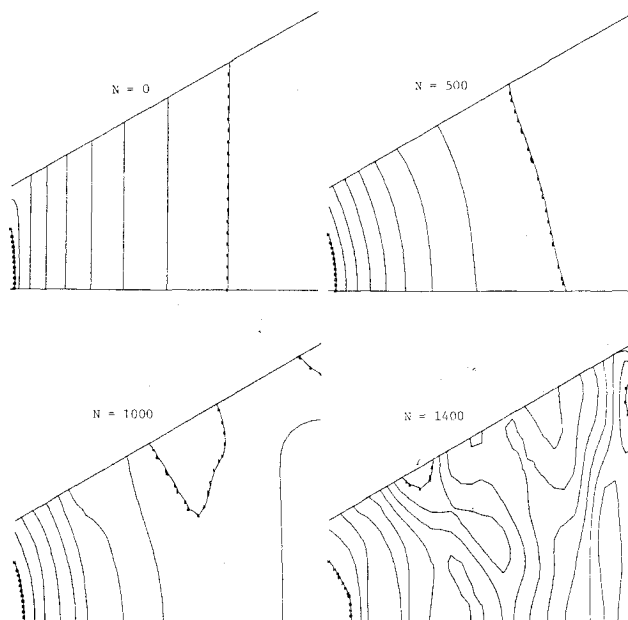


Fig. 4 Mach number contours for the planar source flow case.

the interior of the computational region to the boundary) are satisfied.

As an example, consider the reference plane characteristic theory presented in Ref. 1. These reference plane characteristics are the projection of the true bicharacteristics on the reference planes and, therefore, reduce to the bicharacteristics on the midplane. Four compatibility equations can be written along three bicharacteristics and the streamline to form one set of equations, or two compatibility equations can be written along two bicharacteristics and two compatibility equations along the streamline to form a second set of equations. It is this second set of equations that reduces to the reference plane equations on the midplane. For more details see Ref. 3. In the reference plane characteristic theory,<sup>1</sup> the original continuity,  $x$ -momentum,  $y$ -momentum, and energy equations can be written as four compatibility equations on three characteristics. Specifically, we have one compatibility equation along each of two Mach lines and two compatibility equations along the streamline.

For subsonic inflow, there are three compatibility equations on two incoming characteristics (Mach line and streamline) so three boundary conditions must be specified. Because the compatibility equation for the one outgoing characteristic (Mach line) involves  $u$  and  $p$ , both  $u$  and  $p$  cannot be specified arbitrarily. If we specify  $u$  then  $p$  can be determined from the one compatibility equation. Because we need three boundary conditions,  $v$  and  $\rho$  are specified. Therefore, we can specify  $u$ ,  $v$ , and  $\rho$  to form one possible set of boundary conditions.

For subsonic outflow, there is one compatibility equation for the one incoming characteristic and, hence, one boundary condition. Now there are three compatibility equations on two outgoing characteristics. Because one equation contains  $v$  only, we can calculate  $v$  directly. One equation contains  $u$  and  $p$  and the last equation contains  $p$  and  $\rho$ , so we can specify  $p$  as the one boundary condition and calculate  $u$  and  $\rho$ . Therefore, we can specify  $p$  as one possible boundary condition.

Therefore, according to the above characteristic theory as well as that of Ref. 2, the boundary conditions used here for subsonic inflow and outflow are correct for a well-posed problem. The inviscid fluid model and free-slip wall boundary condition are discussed in Sec. V.

Before leaving the subject of boundary conditions there are two additional points that are worth discussing. The first point is that, so far, we have used characteristic theory to

determine what variables should be specified at the boundaries. How we determine the nonspecified variables is another problem. We could use the outgoing characteristic compatibility equations to determine these variables, which is the procedure used by the VNAP code. However, we could use the original governing equations with one-sided differences normal to the boundary, or use extrapolation or reflection to define values at fictitious grid points. The point here is that once the correct boundary conditions are specified, an accurate and stable numerical procedure is required to determine the nonspecified variables.

The second point concerns the work of Griffin and Anderson,<sup>4</sup> who encountered the same stability problem, exhibited by the source flow calculation, in a quasi-one-dimensional, time-dependent nozzle calculation. According to the characteristic theory, one possible set of boundary conditions for their one-dimensional flow is specifying  $u$  and  $\rho$  for subsonic inflow and  $p$  for subsonic outflow. However, in order to get a stable solution in the downstream diverging portion of the nozzle, they had to overspecify the boundary conditions; that is,  $u$ ,  $p$ , and  $T$  for subsonic inflow and  $p$  and  $T$  for subsonic outflow where  $T$  is temperature. These, however, are not the correct boundary conditions. Had they calculated a purely converging subsonic flow, they would have found that specifying the correct boundary conditions would have produced a stable solution. It is only the diverging or decelerating aspect of subsonic flow that causes the stability problem. The reason Griffin and Anderson were able to get stable solutions by overspecifying the boundary conditions was that they specified the exact solution. In general, one can always overspecify the boundary conditions provided one uses the exact solution, which usually is not known in advance. When overspecifying the boundary conditions without using the exact solution, the solution being approximated generally is not continuous.<sup>2</sup> This point is discussed further in the next section.

In their paper Griffin and Anderson state that "it is important to supply boundary conditions on the computational domain which are appropriate to the steady-state problem" and also that "time-dependent solutions of purely subsonic duct flows require in theory that  $p$ ,  $T$ , and  $u$  be fixed at both the inlet and exit" which gives us six boundary conditions. The theory they refer to is that as the flow approaches steady state, the time derivatives go to zero, and the equations take on an "elliptic nature" and, thus, require Dirichlet boundary conditions. Because they solved the one-dimensional equations, the steady-state equations form a system of three first-order, ordinary differential equations requiring only three boundary conditions, which is the same number required by the time-dependent equations. Therefore, both the steady-state and time-dependent, one-dimensional equations require the same number of boundary conditions.

For two-dimensional, steady-state, subsonic flow, the equations are not purely elliptic but, instead, are a combination of elliptic and hyperbolic since they are two complex characteristics and one real one—the streamline. Note that it is the irrotational equations, and not the Euler equations, that are purely elliptic. For a derivation of these characteristic relations see Ref. 5. Therefore, specifying all variables at both inflow and outflow boundaries (Dirichlet boundary conditions) is not appropriate for the steady-state Euler equations. Because the steady-state equations are not purely hyperbolic, characteristic theory cannot be used to determine the boundary conditions. Correct boundary conditions for the steady-state Euler equations, however, could be determined by the methods of Ref. 2. Because we have not determined the boundary conditions for the steady-state Euler equations for subsonic flow, it is not known whether these equations require additional boundary conditions over the time-dependent equations. (For supersonic flow, the steady-state equations do not require additional boundary conditions over the time-dependent equations). If the steady-state Euler equations for

subsonic flow require the same number of boundary conditions as the time-dependent equations, then there would be no confusion. However, the point is that the procedures discussed above for determining the boundary conditions for the time-dependent equations make no assumptions on the size of the time derivatives. As a result, these procedures give the correct boundary conditions for any flows calculated using the time-dependent equations.

#### IV. Stability Analysis

After determining that the numerical method and boundary conditions do not appear to be causing the source flow instability, the next step was to check the stability of the differential equations. To simplify the work a linear, variable coefficient, stability analysis was applied to the one-dimensional, variable area equations. Although this procedure neglects nonlinear effects, much useful information has been obtained using this method for nonlinear problems.

The one-dimensional, variable area, time-dependent, Navier-Stokes equations can be written as:

Continuity

$$\frac{\partial \rho}{\partial t} + u \frac{\partial \rho}{\partial x} + \rho \frac{\partial u}{\partial x} + \frac{\rho u}{A} \frac{dA}{dx} = 0 \quad (1)$$

Momentum

$$\frac{\partial u}{\partial t} + u \frac{\partial u}{\partial x} + \frac{1}{\rho} \frac{\partial p}{\partial x} = \frac{\mu_2}{\rho A} \frac{\partial}{\partial x} \left( A \frac{\partial u}{\partial x} \right) \quad (2)$$

Energy

$$\frac{\partial p}{\partial t} + u \frac{\partial p}{\partial x} + \gamma p \left( \frac{\partial u}{\partial x} + \frac{u}{A} \frac{dA}{dx} \right) = \mu_1 \left( \frac{\partial u}{\partial x} \right)^2 + \frac{k_1}{A} \frac{\partial}{\partial x} \left( A \frac{\partial T}{\partial x} \right) \quad (3)$$

Equation of state for a perfect gas

$$p = \rho R T \quad (4)$$

$\rho$  is the density,  $u$  the velocity,  $p$  the pressure,  $T$  the temperature,  $A$  the cross sectional area,  $R$  the gas constant,  $\gamma$  the ratio of specific heats,  $\mu_2 = 4\mu/3$ ,  $\mu_1 = (\gamma - 1)\mu_2$ ,  $k_1 = (\gamma - 1)k$ ,  $\mu$  the viscosity,  $k$  the conductivity,  $x$  the distance in the direction of flow, and  $t$  the time.

If we assume that  $\rho = \bar{\rho} + \rho'$ ,  $u = \bar{u} + u'$ ,  $p = \bar{p} + p'$ , and  $T = \bar{T} + T'$ , where the bar and prime denote the steady state and perturbation quantities, respectively, and dropping nonlinear terms, Eqs. (1), (2), and (3) can be written as

$$\frac{\partial \rho'}{\partial t} + \bar{u} \frac{\partial \rho'}{\partial x} + \bar{\rho} \frac{\partial u'}{\partial x} + u' \frac{\partial \bar{\rho}}{\partial x} + \bar{\rho}' \frac{\partial \bar{u}}{\partial x} + \frac{\bar{\rho} u' + \rho' \bar{u}}{A} \frac{dA}{dx} = 0 \quad (5)$$

$$\frac{\partial u'}{\partial t} + \bar{u} \frac{\partial u'}{\partial x} + \frac{1}{\bar{\rho}} \frac{\partial p'}{\partial x} + \frac{\bar{\rho} u' + \rho' \bar{u}}{\bar{\rho}} \frac{\partial \bar{u}}{\partial x} = \frac{\mu_2}{\bar{\rho} A} \frac{\partial}{\partial x} \left( A \frac{\partial u'}{\partial x} \right) \quad (6)$$

$$\begin{aligned} \frac{\partial p'}{\partial t} + \bar{u} \frac{\partial p'}{\partial x} + \gamma \bar{p} \frac{\partial u'}{\partial x} + u' \frac{\partial \bar{p}}{\partial x} + \gamma p' \frac{\partial \bar{u}}{\partial x} \\ + \frac{\gamma \bar{p} u' + \gamma p' \bar{u}}{A} \frac{dA}{dx} = 2\mu_1 \frac{\partial \bar{u}}{\partial x} \frac{\partial u'}{\partial x} + \frac{k_1}{A} \frac{\partial}{\partial x} \left( A \frac{\partial T'}{\partial x} \right) \end{aligned} \quad (7)$$

Assuming the following solutions

$$\rho' = a(x)e^{\alpha t}; \quad u' = b(x)e^{\alpha t}; \quad p' = c(x)e^{\alpha t}; \quad T' = f(x)e^{\alpha t} \quad (8)$$

Eqs. (5-7) become

$$\alpha\alpha + \bar{u} \frac{da}{dx} + \bar{p} \frac{db}{dx} + b \frac{\partial \bar{p}}{\partial x} + a \frac{\partial \bar{u}}{\partial x} + \frac{\bar{p}b + \bar{u}a}{A} \frac{dA}{dx} = 0 \quad (9)$$

$$b\alpha + \bar{u} \frac{db}{dx} + \frac{1}{\bar{p}} \frac{dc}{dx} + \frac{\bar{p}b + \bar{u}a}{\bar{p}} \frac{\partial \bar{u}}{\partial x} = \frac{\mu_2}{\bar{p}A} \frac{d}{dx} \left( A \frac{db}{dx} \right) \quad (10)$$

$$\begin{aligned} c\alpha + \bar{u} \frac{dc}{dx} + \gamma \bar{p} \frac{db}{dx} + b \frac{\partial \bar{p}}{\partial x} + \gamma c \frac{\partial \bar{u}}{\partial x} + \frac{\gamma \bar{p}b + \gamma \bar{u}c}{A} \frac{dA}{dx} \\ = 2\mu_1 \frac{\partial \bar{u}}{\partial x} \frac{db}{dx} + \frac{k_1}{A} \frac{d}{dx} \left( A \frac{df}{dx} \right) \end{aligned} \quad (11)$$

The boundary conditions for Eqs. (1-3) are  $\rho$  and  $u$  specified at the inlet and  $p$  specified at the exit. For Eqs. (9-11) the boundary conditions become

$$x=0, \quad a=b=0 \quad (12)$$

$$x=L, \quad c=0 \quad (13)$$

Thus, Eqs. (9-13), along with Eq. (4), form a two-point boundary value problem.

This boundary value problem was solved using the following finite-difference procedure.  $L=1$  to  $L_{MAX}$  uniformly spaced grid points were specified on the  $x$  axis. At each grid point the solution for the steady-state inviscid equations, which is also the exact solution for the midplane of the source and sink flows, was determined. This solution was used to determine the coefficients in Eqs. (9-11) at each grid point. The derivatives of the flow variables in these coefficients were determined using centered finite differences. Next, the derivatives of  $a$ ,  $b$ , and  $c$  were replaced by centered finite differences. The unknown  $f$  in Eq. (11) was eliminated using the equation of state. At the two boundaries, one-sided differences were used. This produced a set of  $3 \cdot L_{MAX} - 3$  homogeneous algebraic equations for the  $3 \cdot L_{MAX} - 3$  unknowns,  $c_1, a_2, b_2, c_2, \dots, a_{L_{MAX}-1}, b_{L_{MAX}-1}, c_{L_{MAX}-1}, a_{L_{MAX}}, b_{L_{MAX}}$ . The values  $a_1, b_1$ , and  $c_{L_{MAX}}$  are zero due to the boundary conditions and, therefore, Eqs. (9) and (10) at  $L=1$  and Eq. (11) at  $L=L_{MAX}$  are not solved. For this set of equations to have a nontrivial solution the determinant of the coefficient matrix must vanish. Because the  $\alpha$ 's are on the diagonal, their solution reduces to an eigenvalue problem for a real matrix. As a result, a standard eigenvalue routine was used to generate the  $\alpha$ 's.

Figure 5 is a plot of  $\alpha$ 's in the complex plane for inviscid sink and source flow. Since the  $\alpha$ 's were either real or complex conjugate pairs, only the positive imaginary axis is plotted. In addition, all the  $\alpha$  curves are envelopes of  $\alpha$ , that is, there are no  $\alpha$ 's to the right of the curves. From Fig. 5, we see that both flows have some  $\alpha$ 's with real parts greater than zero and are, therefore, unstable. Figure 6 gives the  $\alpha$ 's for values of viscosity and conductivity that are 12 times the laminar values. From Fig. 6, we see that the sink flow now has the real part of all  $\alpha$ 's less than zero and is stable. However, the source flow still has some  $\alpha$ 's with real parts greater than zero. Increasing the viscosity further did not change this result.

Therefore, the source flow is physically unstable, whereas the sink flow is conditionally stable. Because the numerical viscosity for the sink flow calculation presented in Sec. I is at least 12 times the laminar value, the stable numerical result is consistent with the results of this stability analysis. However, this conditional stability result indicates that for a high enough Reynolds number perturbations grow and the flow becomes unstable. This is essentially what happens in real flows. That is, above a critical Reynolds number, perturbations grow and the flow becomes turbulent. The fact that the growth of these perturbations is bounded is due to the

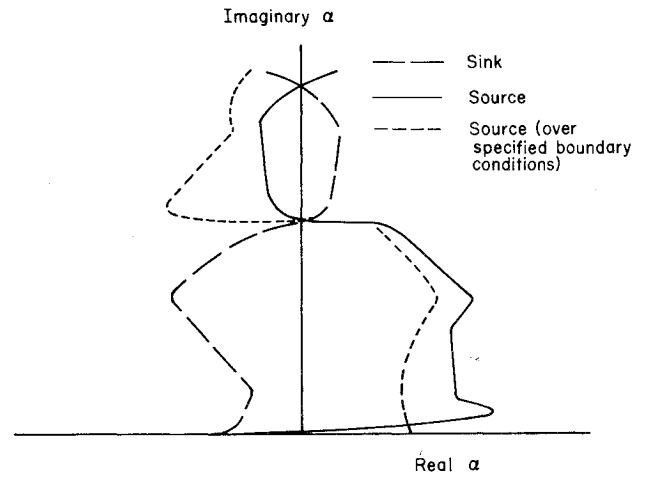


Fig. 5 Plot of  $\alpha$  in the complex plane for the source and sink flows.

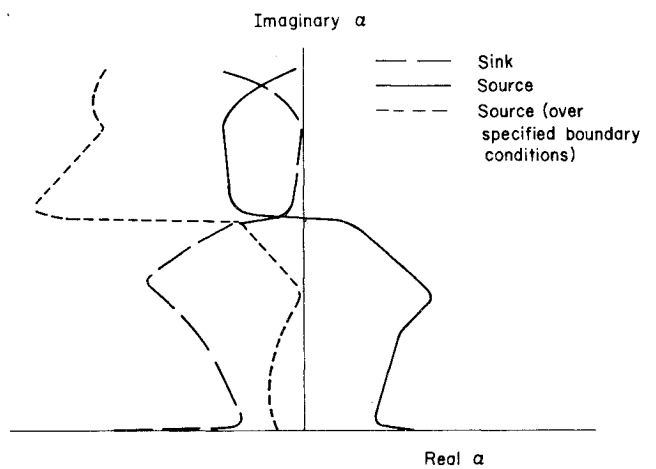


Fig. 6 Plot of  $\alpha$  in the complex plane for the source and sink flows with nonzero viscosity and conductivity.

nonlinear terms not considered by this linear stability analysis. In fact, the turbulent fluctuations enhance the effective viscosity, which reduces the Reynolds number. As a result, there are high Reynolds number flows where perturbations do grow, but the mean flow is stable. Therefore, while this linear, one-dimensional analysis is not capable of predicting the onset of turbulence, it does indicate that perturbations grow above a critical Reynolds number. It should be noted that the results shown in Figs. 5 and 6 were calculated using 121 grid points. Calculations also were made with 31 and 61 grid points. As the number of grid points increased, the amount of viscosity required to stabilize the sink flow decreased. However, the limiting value of viscosity as  $\Delta x$  goes to zero was not determined. The main point is that with some dissipation converging flows are stable while diverging flows are unstable regardless of the amount of dissipation.

We can overspecify the source flow boundary conditions, as done by Griffin and Anderson,<sup>4</sup> by specifying  $\rho$ ,  $u$ , and  $p$  at the inlet and  $p$  and  $\rho$  at the exit. To determine the  $\alpha$ 's, we drop the equations for  $c_1$  and  $a_{L_{MAX}}$  and calculate the eigenvalues of the remaining  $3 \cdot L_{MAX} - 5$  equations. The  $\alpha$ 's for the inviscid case are given in Fig. 5, whereas those, where the viscosity and conductivity are 39 times the laminar values, are shown in Fig. 6. Since the real part of all  $\alpha$ 's in Fig. 6 is less than zero, overspecifying the boundary conditions will stabilize the flow. To check the effect of these additional boundary conditions on the two-dimensional numerical

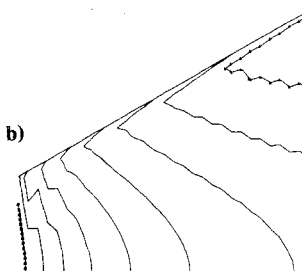
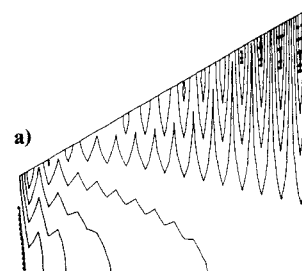
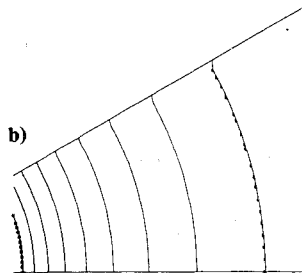
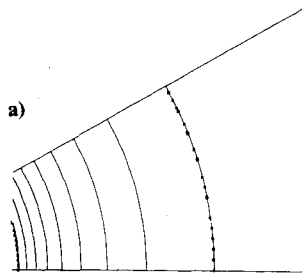


Fig. 7 Source flow case with exact overspecified boundary conditions,  $N=3000$ ; a) density contours, b) Mach number contours.

Fig. 8 Source flow case with approximate overspecified boundary conditions,  $N=3000$ ; a) density contours, b) Mach number contours.

results, the source flow calculation was repeated specifying  $u$ ,  $v$ ,  $p$ , and  $\rho$  at the inflow boundary and  $\rho$  and  $p$  at the outflow boundary where all specified values are the exact solution. The density and Mach number contours for  $N=3000$  are shown in Fig. 7. From Fig. 7, we see that the additional boundary conditions considerably improved the flow stability. Next, the source flow solution was repeated with the value of  $p$  at the inflow and  $\rho$  at the outflow boundary set equal to a uniform value instead of the exact solution. The uniform value chosen was the exact solution midplane value. The results of this calculation are shown in Fig. 8. From Fig. 8, we see that this reasonable, but not exact solution, boundary condition did not produce a reasonable solution. Therefore, we see that overspecifying the boundary conditions will stabilize the flow, however, if we do not use the exact solution, we may get a physically unreasonable solution.

As a final footnote to the stability analysis, there is the question of whether the finite-difference procedure used to solve the linear perturbation equations affects the stability results. This solution procedure is equivalent to first discretizing the perturbation equations in space and then substituting in Eq. (8), where now the functions  $a$ ,  $b$ ,  $c$ , and  $f$  are defined at the grid points. In order to check the effect of

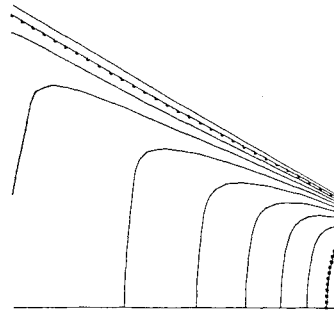


Fig. 9 Mach number contours for the viscous "sink" flow case,  $N=3000$ .

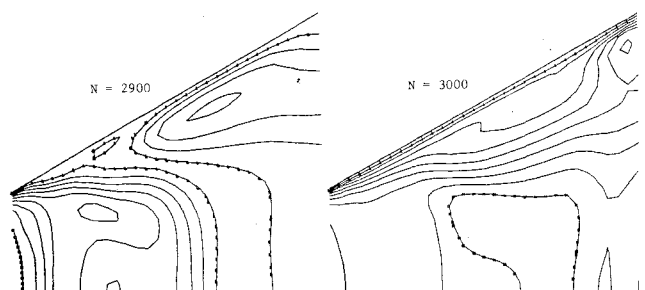
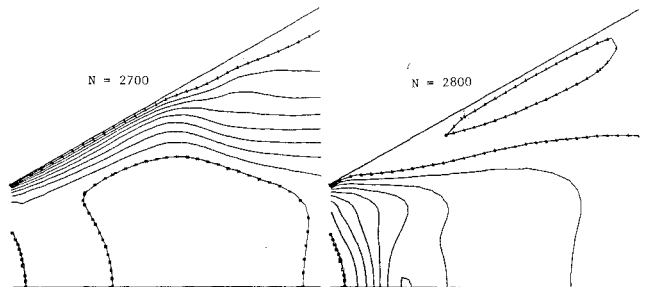


Fig. 10 Mach number contours for the viscous "source" flow case.

the finite-difference procedure, three simple, linear prototype equations, the convection, wave, and heat equations, were studied. All three equations were discretized in space using centered differences and the stability of the continuous time derivatives was checked. The convection and wave equations had an  $\alpha$  that was purely imaginary and, therefore, were neutrally stable. The heat equation had an  $\alpha$  with a negative real part and therefore, was stable. As a result of these heuristic arguments, it is felt that the finite-difference procedure has little effect on the results of the stability analysis.

## V. Viscous Flow

Because the linear stability analysis showed the source flow to be physically unstable, it was decided to try removing the inviscid flow and free-slip wall assumptions. The same grid point distribution and inflow and outflow boundary conditions used for the sink and source flows were used. However, the inlet values of  $u$  and  $v$  at the last few grid points near the wall were modified to simulate a boundary layer profile. Reynolds and Prandtl numbers of 100 and 0.71, respectively, were assumed. The viscous "sink" flow Mach number contours for  $N=3000$  are shown in Fig. 9. From Fig. 9, we see that the central, mostly inviscid, part of the flow closely resembles the sink flow results. In fact, by diverging the wall an amount equal to the boundary layer displacement thickness, the sink flow results could be closely approximated.

Figure 10 presents the viscous "source" flow Mach number contours for  $N=2700$ , 2800, 2900, and 3000. From Fig. 10, we see that the central part of this flow does not resemble the

source flow results. In fact, Fig. 10 shows one cycle of an unsteady process where the boundary layer separates from the wall, a recirculation region develops, and finally the flow reattaches. This process comes as no surprise for anyone familiar with subsonic diffusers. In fact a discussion of this flow situation is given in Ref. 6. The boundary layer usually separates for wall divergence angles greater than 5-7 deg.<sup>6</sup> Where the recirculating flow causes inflow at the outflow boundary, the VNAP code automatically enforces inflow boundary conditions. In addition, the code automatically applied the additional viscous boundary conditions.<sup>2</sup>

In conclusion, the source flow case or more generally inviscid, subsonic flow in a diverging duct does not approximate in any way the real separated viscous flow. The main shortcoming of the inviscid flow model is the free-slip wall boundary condition, since simply adding the viscous terms to a free-slip wall calculation produces no improvement. Therefore, it should not come as a surprise that the inviscid source flow results were unstable.

## VI. Recommendations

Since the use of an inviscid flow model to calculate diverging subsonic flow does not model in any way the true separated viscous flow, its use should be avoided. Using overspecified boundary conditions in order to stabilize an inviscid calculation would be nonproductive.

Such diverging flows occur in such obvious places as subsonic diffusers and inlets. However, they also occur in supersonic nozzles downstream of a normal shock. The presence of this shock could be due to a high back pressure or a downstream flow obstruction such as those that occur in rocket interstaging. As pointed out by one of the reviewers, such flows also occur "just downstream of the shock wave in the transonic flow field about an airfoil." It should be mentioned that the viscous flow results presented here are for

laminar flow whereas in many cases the boundary layer downstream of the shock is turbulent and, therefore, less likely to separate. However, similar boundary-layer separation properties have been observed for turbulent boundary layers.<sup>6</sup> Also, the shock itself may cause the boundary layer to separate. Finally, predicting whether or not the boundary layer separates is beyond the capability of most boundary-layer codes used in an inviscid analysis.

## Acknowledgement

This work was supported by the Propulsion Aerodynamics Branch of the NASA Langley Research Center, Hampton, Va., and performed under the auspices of the U.S. Dept. of Energy. The author wishes to thank F. H. Harlow, R. C. Mjolsness, and J. D. Ramshaw of the Los Alamos Scientific Laboratory for their many helpful discussions.

## References

- <sup>1</sup>Cline, M. C., "VNAP: A Computer Program for Computation of Two-Dimensional, Time-Dependent Compressible, Viscous, Internal Flow," Los Alamos Scientific Laboratory, Rept. LA-7326, Nov. 1978.
- <sup>2</sup>Oliger, J. and Sundström, A., "Theoretical and Practical Aspects of Some Initial Boundary Value Problems in Fluid Dynamics," *SIAM Journal of Applied Mathematics*, Vol. 35, Nov. 1978, pp. 419-446.
- <sup>3</sup>Rusanov, V. V., "The Characteristics of General Equations of Gas Dynamics," *Zhurnal Vychislitel'noi Matematiki i Matematicheskoi Fiziki*, Vol. 3, No. 3, 1963, pp. 508-527.
- <sup>4</sup>Griffin, M. D. and Anderson, J. D. Jr., "On the Application of Boundary Conditions to Time Dependent Computations for Quasi One-Dimensional Fluid Flows," *Computers and Fluids*, Vol. 5, Sept. 1977, pp. 127-137.
- <sup>5</sup>Hoffman, J. D., "Accuracy Studies of the Numerical Method of Characteristics for Axisymmetric, Steady Supersonic Flows," *Journal of Computational Physics*, Vol. 11, Feb. 1973, pp. 210-239.
- <sup>6</sup>Schlichting, H., *Boundary-Layer Theory*, Sixth Edition, McGraw-Hill Book Co., N.Y., 1968, pp. 99, 100, 626-628.

## *From the AIAA Progress in Astronautics and Aeronautics Series . . .*

# **AEROACOUSTICS: FAN, STOL, AND BOUNDARY LAYER NOISE; SONIC BOOM; AEROACOUSTIC INSTRUMENTATION—v. 38**

*Edited by Henry T. Nagamatsu, General Electric Research and Development Center; Jack V. O'Keefe, The Boeing Company; and Ira R. Schwartz, NASA Ames Development Center*

*A companion to Aeroacoustics: Jet and Combustion Noise; Duct Acoustics, volume 37 in the series.*

Twenty-nine papers, with summaries of panel discussions, comprise this volume, covering fan noise, STOL and rotor noise, acoustics of boundary layers and structural response, broadband noise generation, airfoil-wake interactions, blade spacing, supersonic fans, and inlet geometry. Studies of STOL and rotor noise cover mechanisms and prediction, suppression, spectral trends, and an engine-over-the-wing concept. Structural phenomena include panel response, high-temperature fatigue, and reentry vehicle loads, and boundary layer studies examine attached and separated turbulent pressure fluctuations, supersonic and hypersonic.

Sonic boom studies examine high-altitude overpressure, space shuttle boom, a low-boom supersonic transport, shock wave distortion, nonlinear acoustics, and far-field effects. Instrumentation includes directional microphone, jet flow source location, various sensors, shear flow measurement, laser velocimeters, and comparisons of wind tunnel and flight test data.

509 pp. 6 x 9, illus. \$19.00 Mem. \$30.00 List

TO ORDER WRITE: Publications Dept., AIAA, 1290 Avenue of the Americas, New York, N. Y. 10019